

PHYSICAL REVIEW B

CONDENSED MATTER

THIRD SERIES, VOLUME 28, NUMBER 6

15 SEPTEMBER 1983

Structure of glassy early-transition-metal-late-transition-metal hydrides

K. Samwer* and W. L. Johnson

W. M. Keck Laboratory of Engineering, California Institute of Technology, Pasadena, California 91125

(Received 7 March 1983)

Hydrogen is used as a probe for obtaining structural information on metallic glasses. Results from experimental radial distribution functions of hydrided and unhydrided Zr_3Rh and Zr_2Pd glasses show a significant change in the nearest-neighbor distance of Zr atoms. The measured distance suggests that hydrogen occupies mainly tetrahedral sites defined by four Zr atoms under normal hydriding conditions (1 atm H_2 , $\sim 200^\circ C$). A statistical model for these sites based on current dense-random-packing models is in good agreement with the observed absorption capacity for hydrogen. We predict that H-H interaction should limit the upper value of hydrogen content in Zr-based glasses to 2.5 (H/metal atom).

I. INTRODUCTION

Amorphous metallic hydrides have become of general interest as potential hydrogen-storage materials and for other applications. Recently, reaction with hydrogen was also used to transform certain intermetallic compounds into amorphous material by a solid-state reaction.¹ This opens the field for a new class of amorphous metallic materials produced without any rapid solidification technique. Despite these interesting technological aspects, the nature of the interaction of hydrogen in amorphous metals, especially of the transition-metal series, is still unknown. It is of particular importance to determine the location of hydrogen sites and the nature of the local environment of hydrogen atoms in glassy material. In this paper, we present x-ray diffraction experiments on hydrided and unhydrided Zr-based metallic glasses as well as a structural model for hydrogen absorption capacity based on the current knowledge of the microstructure of glassy metals. Severe restrictions for a minimal H-H interaction distance already known for crystalline metallic hydrides will be considered which may lead to an upper limit for absorption of hydrogen in metallic glasses.

II. EXPERIMENTAL

The Zr-Rh and Zr-Pd alloys for the present investigation were prepared by levitation melting on a silver boat in purified argon atmosphere. The ingots are remelted several times to assure a homogeneous sample. Amorphous Zr-Pd ribbons were then produced by the melt spin-

ning technique² in a pure He-gas atmosphere. The ribbons have an average thickness of about 20–40 μm . Amorphous Zr_3Rh samples were made mainly by rapid quenching using a piston and anvil technique³ in the form of (30–50)- μm -thick foils. The structure of all samples was checked by x-ray diffraction using $CuK\alpha$ radiation. Hydrogen was introduced into the amorphous ribbons at pressures either below one atmosphere of H_2 gas or up to 50 atmospheres in two different stations. All hydrides for which data are presented were made at a temperature of $180^\circ C$. The amount of hydrogen absorbed by the sample was measured by observing the change of H_2 pressure in a known volume and/or by the change in sample weight. The latter method has a much lower accuracy due to problems with sample surface oxidation. The thin oxide layer formed when the hydrided samples were exposed further to air was observed to act to seal the sample surface against hydrogen permeation.

The mass density was measured using Archimedes method with toluene as the working fluid. The structure factor of the hydrided and unhydrided Zr-based amorphous alloys was measured using a vertical Norelco diffractometer in reflection mode with $MoK\alpha$ radiation and a focusing LiF monochromator in the diffracted beam. The data were corrected for background, polarization, and Compton scattering using the standard procedures⁴ to obtain the reduced radial distribution function $G(r) = 4\pi r[\rho(r) - \rho_0]$.

The superconducting transition temperature T_c of the hydrided samples was measured resistively in a 3He cryostat which has a lower temperature limit of about 0.4 K. For the unhydrided samples, T_c was determined by an inductive measurement in a standard 4He cryostat.

III. RESULTS

The absorption of hydrogen in amorphous Zr_2Pd and Zr_3Rh metals was observed at temperatures of $180^\circ C$. As earlier reported,^{1,5} no crystallization of the samples (as determined by high-angle x-ray scattering) could be detected. The amount of hydrogen absorbed by the samples was observed to be slightly pressure dependent.⁶ At a pressure just below 1 atm a final hydrogen-to-metal ratio of $[H]/[M] \cong 0.91 \pm 0.02$ was determined for amorphous a - Zr_2Pd . With hydriding an alloy density change from 8.02 g/cm^3 for a - Zr_2Pd to 7.19 g/cm^3 for a - $Zr_2Pd_{1.7}H_{2.7}$ is observed.⁵ This indicates an expansion of 13% in volume during hydrogenation. Although all hydrided samples were found to be extremely brittle, they maintained their physical integrity. An attempt was made to introduce more hydrogen in a - Zr_2Pd by hydriding at pressures up to 25 atm. Unfortunately, the accuracy of measuring changes in the pressures during hydrogenation was very low at high pressure. Therefore, the $[H]/[M]$ ratio determined by weighing was $[H]/[M] \cong 1.0 \pm 0.1$. (The uncertainty is much higher here because of the difficulty handling these brittle materials for weighing.)

Amorphous Zr_2Pd has a superconducting transition temperature T_c of $T_c = 2.45 \text{ K}$. After annealing the sample for 11 h at $190^\circ C$, T_c drops to $T_c = 2.17 \text{ K}$ with a transition width of $\Delta T_c \cong 70 \text{ mK}$ (ΔT_c is defined as the change in T between 10% and 90% of the full transition). Introducing hydrogen decreases T_c even more. For 23 at. % H in Zr_2Pd , two steps in the superconducting transition were found.⁵ For amorphous $Zr_2PdH_{2.7}$ this behavior was clearly seen in two steps at $T_{c1} \cong 1.23$ with $\Delta T_c \cong 0.18 \text{ K}$ and $T_{c2} \cong 0.68 \text{ K}$ with a $\Delta T_c \leq 10 \text{ mK}$. These results suggest that the material consists of two slightly different superconducting phases. This might be caused by an inhomogeneous hydrogen density in this alloy. As we show later, no evidence for phase separation could be found in x-ray diffraction experiments.

Figure 1 shows the reduced interference function, $i(K) = k[I(K) - 1]$, for four different states of a - Zr_2Pd . The as-quenched sample shows the typical behavior of a metal-metal glass with pronounced shoulder of the second peak and less structure at higher K values. With annealing at $190^\circ C$, the position of the first peak moves about 3% to the lower K side whereas the height increases slightly. Hydriding at 1 atm H_2 shifts the main peak another 2.5% to lower K and reduces the height. Note that also the second peak changes in height relative to the shoulder, whereas slightly more features occur at higher k values. High-pressure hydriding shifts the position of the main peak less than 1% to lower k values but reduces the height rapidly. The second peak is now almost smeared out into a broad plateau.

Figure 2 shows the reduced radial distribution function $G(r)$ obtained from

$$G(r) = \frac{2}{\pi} \int_0^{K_{\max}} K [I(K) - 1] \sin(Kr) e^{-\alpha K^2} dK$$

for all four alloys in the same way. For the Fourier transform the usual convergence factor $e^{-\alpha K^2}$ (Ref. 4) was introduced to reduce the ripples coming from the termina-

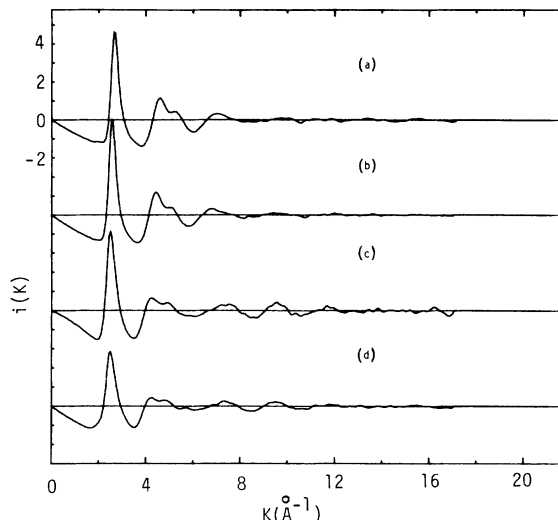


FIG. 1. Reduced interference functions $i(K) = k[I(K) - 1]$ obtained from x-ray diffraction for (a) as-quenched Zr_2Pd , (b) as-quenched Zr_2Pd followed by an anneal at $190^\circ C$ for 11 h, (c) $Zr_2PdH_{2.7}$ prepared in 1 atm of H_2 at $180^\circ C$, and (d) $Zr_2PdH_{3.0}$ prepared in 25 atm of H_2 at $180^\circ C$.

tion of the integral at $K_{\max} \cong 17.7 \text{ \AA}^{-1}$ for $MoK\alpha$ radiation. All data are processed with $\alpha = 0.005$ to allow comparison between them. In the case of the hydrided samples this leads to some unphysical ripples in the $G(r)$. For interpretation of the data, we restrict ourselves therefore to the main peak. For as-quenched Zr_2Pd the average nearest-neighbor distance was found to be $r_1 = 2.90 \text{ \AA}$ and rather broad. This seems to indicate that the main peak consists of an average of Zr-Zr and Zr-Pd nearest neighbors, which indeed give the main contribution to the average $G(r)$. With annealing, the position of the main peak shifts to a higher value (see Table I), which could indicate a chemical redistribution of nearest neighbors in addition

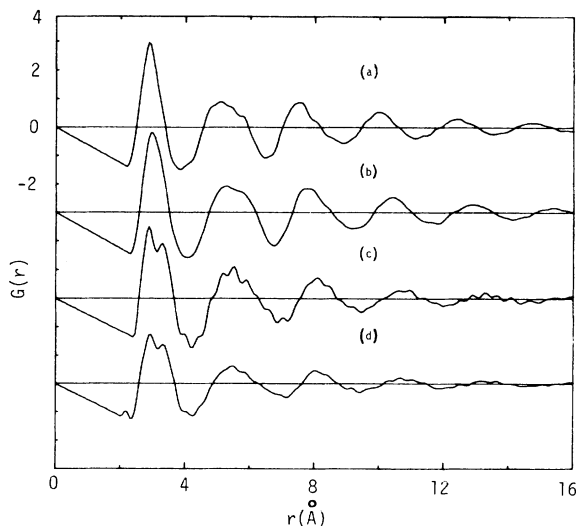


FIG. 2. Reduced radial distribution functions $G(r) = 4\pi r[\rho(r) - \rho_0]$, obtained from x-ray interference functions for (a) as-quenched Zr_2Pd , (b) as-quenched Zr_2Pd followed by anneal at $190^\circ C$ for 11 h, (c) $Zr_2PdH_{2.7}$ prepared in 1 atm of H_2 at $180^\circ C$, and (d) $Zr_2PdH_{3.0}$ prepared in 25 atm of H_2 at $180^\circ C$.

TABLE I. Experimental data from different Zr-based amorphous metals.

| | r'_1 | r_1 | $\frac{r'_2}{r_1}$ | $\frac{r_2}{r_1}$ | ρ | T_c | ΔT_c | c^a |
|-----------------------------------------------|--------|-------|--------------------|-------------------|----------------------|--------------|-----------------------------------|-------|
| | (Å) | | | | (g/cm ³) | (K) | (10 ⁻³ K) ^a | |
| Zr ₂ Pd | | 2.90 | | 1.76 | 8.02 | 2.45 | 20 | |
| Zr ₂ Pd annealed 11 h ~190°C | | 2.97 | | 1.77 | 8.02 | 2.17 | 70 | |
| Zr ₂ PdH _{2.73} | 2.89 | 3.32 | 1.78 | 1.65 | 7.19 | 1.23 0.68 | 180 < 10 | 0.91 |
| Zr ₂ PdH _{3.0} | 2.92 | 3.33 | 1.76 | 1.62 | 7.19 | | | 1.0 |
| Zr ₃ Rh | | 3.14 | | 1.75 | 7.58 | 4.40 | 23 | |
| Zr ₃ RhH _{5.5} | 2.93 | 3.35 | 1.78 | 1.68 | 6.54 | 1.22 | 100 | 1.39 |

^aEquilibrium [H]/[M] ratio at pressure of 1 atm (H_c) and $T = 180^\circ\text{C}$.

to normal topological relaxation, which generally leads to a decrease of the nearest-neighbor distance. With hydriding the main peak splits into two subpeaks at $r'_1 \cong 2.89$ Å and $r_1 \cong 3.32$ Å. This is in excellent agreement with values earlier reported on $\text{Zr}_{0.65}\text{Pd}_{0.35}\text{H}_{1.01}$.⁷ From the known Goldschmidt radii, one can assume that Zr-Pd correlations contribute to the lower subpeak while Zr-Zr correlations are dominant at the higher subpeak. One cannot completely rule out the possibility that this splitting might be associated with inhomogeneities. The previously mentioned superconducting measurements suggest a somewhat inhomogeneous distribution of hydrogen. On the other hand, the subpeak positions suggest pair distances which are consistent with Zr-Pd and Zr-Zr pairs. It is difficult to see how inhomogeneities could lead to regions with only Zr-Zr pairs and Zr-Pd pairs, respectively. The same splitting is seen in $\text{Zr}_3\text{RhH}_{5.5}$ (see below) where no inhomogeneity is indicated by superconducting measurements. This suggests the splitting is in fact a result of expansion Zr-Zr distances in the hydride coupled with little change in Zr-Pd distances. Owing to the negligibly small x-ray form factor of hydrogen, direct contributions of hydrogen metal pairs are not observed. Under high hydrogen pressure and therefore slightly higher H concentration, the lower subpeak also begins to move up, while the position of the higher subpeak remains the same within the uncertainty of the measurement. The relative heights of the two subpeaks also changes to a nearly equal value indicating that the number of pairs contributed by each separate peak is becoming nearly equal.

Amorphous Zr_3Rh hydrides can be formed by hydriding either metastable crystalline or amorphous Zr_3Rh . As earlier reported,¹ both hydrides seem to have nearly identical physical properties. For an exact comparison, we restrict our attention here to the hydride made from an initially glassy alloy. The amount of hydrogen absorbed by Zr_3Rh was found to be $c = [\text{H}]/[\text{M}] = 1.39 \pm 0.02$ as measured by change in pressure. The hydriding process was observed to reach equilibrium at 1 atm H_2 gas and 180°C after about five days after which no further change in pressure was noted. The sample density drops from about 7.58 to 6.54 g/cm³ during hydriding, which indicates again an expansion of sample volume of about 13%.

The superconducting transition temperature drops from the as-quenched state value of $T_c \cong 4.40$ K after annealing

(1h, 280°C) by 0.2–0.3 K.⁸ With introduction of hydrogen, T_c drops for a hydrogen content of $c = [\text{H}]/[\text{M}] \cong 0.3$ to $T_c \cong 3.7$ K with a very broad transition ($\Delta T_c \cong 1.4$ K). For a hydrogen content of $c \cong 0.6$, T_c drops even more to $T_c \cong 3.28$ K with again a broad transition of $\Delta T_c \cong 0.88$ K. This broad transition indicates that the distribution of hydrogen is not entirely homogeneous. For a fully hydrided sample with $c = [\text{H}]/[\text{M}] = 1.39$, a measured $T_c = 1.22$ K was obtained with a somewhat narrower transition width of $\Delta T_c = 100$ mK.

Figure 3 shows the reduced interference function for as-quenched Zr_3Rh and $\text{Zr}_3\text{RhH}_{5.5}$. With hydriding, the position of the main peak shifts about 6% to the lower K, but again about 3% of this shift can be attributed to relaxation effects,⁸ which are not separated here. A shift in position and a change in height can also be seen in the second peak. The relative height of the second peak compared to the shoulder is especially changed with hydriding.

The reduced radial distribution function $G(r)$ for the same alloys is shown in Fig. 4. In the as-quenched state the main peak is centered around $r_1 = 3.14$ Å. The large width of the peak suggests that Zr-Zr and Zr-Rh pairs

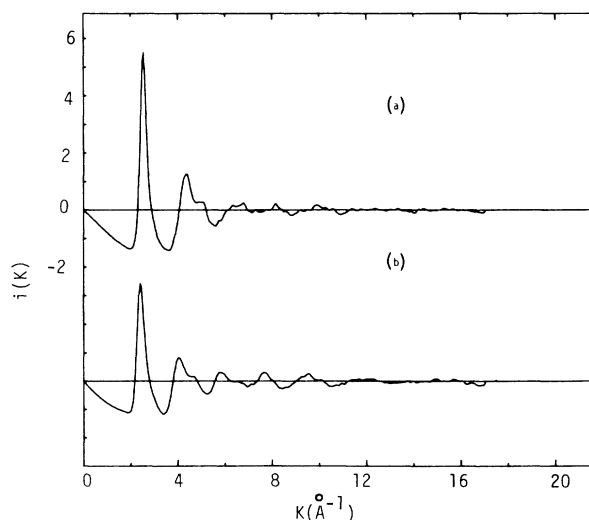


FIG. 3. The reduced interference functions $i(K) = K[I(K) - 1]$ for (a) as-quenched Zr_3Rh and (b) $\text{Zr}_3\text{RhH}_{5.5}$ prepared in 1 atm H_2 at 180°C .

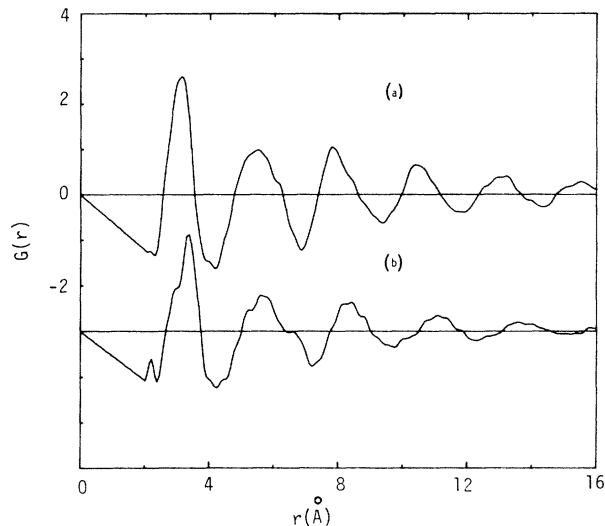


FIG. 4. The reduced radial distribution function $G(r) = 4\pi r[\rho(r) - \rho_0]$ for (a) as-quenched Zr_3Rh and (b) $Zr_3RhH_{5.5}$ prepared in 1 atm H_2 at 180°C.

both contribute to the peak and are not resolved in this measurement. With hydriding the main peak again splits into the separate subpeaks. The subpeak at lower r is observed as a pronounced shoulder with the present resolution and is located at $r_1' = 2.93$ Å, whereas the position of the peak at higher r value is $r_1 = 3.35$ Å. From the known Goldschmidt radii of Rh and Zr and the expected weight factors for various pairs,⁴ one can assume that Zr-Rh atomic pairs are mainly responsible for the subpeak at lower r values, whereas mainly Zr-Zr atomic pairs contribute to the peak at higher r values. As was seen in the $G(r)$ of $Zr_2PdH_{2.7}$, the hydrogen absorption process at 1 atm H_2 pressure leads to a large increase in the Zr-Zr nearest-neighbor distance but does not appear to affect the nearest-neighbor distance between unlike atomic pairs. This difference in the relative expansion of interatomic-pair distances accounts for the splitting of the main peak. The $G(r)$ of $Zr_2RhH_{5.5}$ also shows more features at higher r values. The second peak has much more structure and an attempt can be made to attribute the different subpeaks to simple well-known combinations of interatomic distances in a dense-random-packing model of two sizes of hard spheres by considering the splitting of the main peak.¹ On the other hand, this analysis is limited by the ripples arising from termination at the maximum K value as discussed earlier. We therefore again concentrate our discussion on the results obtained for the main peaks in $G(r)$.

IV. DISCUSSION

As we mentioned earlier, we will try to show that the observed amount of hydrogen absorbed by the Zr-based early-transition-metal-late-transition-metal glasses can be explained in a statistical model where hydrogen occupies tetrahedral sites consisting of four Zr atoms. This description will be limited to hydrides formed at 1 atm H_2 . At higher pressures, other less energetically favorable

hydrogen sites may be occupied. Thus our description focuses on the most favorable hydrogen sites available for occupancy.

Our description is based on the simple observation that under normal conditions (1 atm $H_2 \sim 200^\circ C$), the $G(r)$ functions of the hydrided Zr_2Pd and Zr_3Rh both show a change in the Zr-Zr nearest-neighbor distance, but apparently little or no observable change in the Zr- X (X indicates late transition metal) distance. This provides evidence that the large negative heat of mixing between Zr and H, observed for pure crystalline Zr hydrides,⁹ seems to be the dominant driving force for the reaction. As a second point, we observe in the reduced radial distribution function $G(r)$ nearly the same Zr-Zr distance after hydrogenation for Zr_2Pd as well as for Zr_3Rh . This distance, roughly $r = 3.35$ Å, is nearly the same as the nearest-neighbor Zr distance in fcc ZrH ($r = 3.37$ Å) and in tetragonally distorted δ - ZrH_2 ($r = 3.3-3.49$ Å).¹⁰ In crystalline ZrH and ZrH_2 , hydrogen occupies tetrahedral sites defined by four neighboring Zr atoms. When the pressure of H_2 during hydriding was increased by an order of magnitude in the case of Zr_2Pd , we also observed that the Zr-Pd nearest-neighbor distance begins to increase. Under high-pressure conditions, hydrogen is forced to occupy less energetically favorable interstitial sites, which now can be defined by both Zr and Pd atoms. Since pure crystalline Pd forms a stable hydride with octahedral interstitial hydrogen sites,⁹ one might expect that such mixed sites could become available for hydrogen in amorphous Zr_2Pd . On the other hand, it is well known that the occurrence of octahedra in amorphous metals is very uncommon compared with the occurrence of tetrahedral sites. The interstitial sites in model amorphous structures consist mainly of tetrahedra and higher coordinated Bernal holes.¹¹ Therefore it seems to be likely that tetrahedra, defined by four Zr atoms, are initially occupied by hydrogen atoms as the concentration of hydrogen (or external H_2 pressure) is increased. As will be seen later, the occupancy of all such sites may be forbidden by other considerations. Thus with increasing H_2 pressure, other sites defined by three Zr and one Pd atom, for example, may become occupied. These sites are characterized by a higher internal energy and thus a smaller heat of formation with hydrogen and consequently are not occupied under normal conditions (lower H_2 pressure). Recent nuclear magnetic resonance (NMR) measurements on hydrided Zr_2Pd in both the crystalline and amorphous state support our description in that these measurements suggest that hydrogen atoms preferentially occupy Zr_4 tetrahedral sites.¹² By comparison of NMR spectra of amorphous and crystalline Zr_2Pd hydrides, it was concluded that some octahedral hydrogen sites might also be filled in the amorphous hydride although it seemed to be difficult to distinguish, in the NMR experiments, between an octahedral site and a tetrahedral site consisting of three Zr and one Pd atom. It is worthwhile noting that previous studies of crystalline hydrides of $ZrNi$ show that a counting of the available sites for a given structure can correctly predict the hydrogen concentration¹³ achieved by hydriding at various pressures.

For a calculation of the amount of hydrogen absorbed, we first consider the number of tetrahedra per atom in

various structures. In a dense-random-packing model of hard spheres (DRPHS) the predominant interstitial polyhedra found are tetrahedra (*t*), octahedra (*o*), tetragonal dodecahedra (TD), and finally trigonal prisms (TG) and Archimedean antiprisms (AA) both capped with half octahedra.¹¹ The other interstitials found consist of a very small number of even more complex polyhedra. In a pure topological argument, it can be shown that the latter four polyhedra mentioned above can each be broken down into distorted tetrahedra.¹⁴ For example, an octahedron can be viewed as made up of four distorted tetrahedra. One octahedron plus three tetrahedra form a TD. One *td* plus two *t* form a TP. One TP and two *t* form one AA. Thus the actual number of tetrahedral sites in a DRPHS model far exceeds the number of "pure" tetrahedra when one includes distorted tetrahedra obtained by decomposition of the more complex Bernal holes. In the Bernal model, it was found that the number of pure tetrahedra was 2.5 *t*/atom account for 40.3% of the interstitial volume.¹¹ Using the decomposition of higher polyhedra mentioned above, the total number of tetrahedra per atom in a space filling model would be 6.2 *t*/atom.

This number of tetrahedra per atom can also be roughly obtained in other packing schemes. A packing of icosahedral atomic clusters (Kasper CN12 polyhedra), which cannot fill space due to the fivefold coordination, gives 5 *t*/atom. The σ phase, built from a ratio of three Kasper CN12 to two Kasper CN14 polyhedra, allows $0.6 \times 5 + 0.4 \times 6 = 5.4$ *t*/atom. The MgZn₂ Laves phase, consisting of two Kasper CN12 and one Kasper CN16, has $0.66 \times 5 + 0.33 \times 7 = 5.66$ *t*/atom. Note that the interstitial space in fcc and bcc phases can also be divided into 6 *t*/atom by decomposition of octahedra into tetrahedra.

For the purpose of calculation in our statistical model, we choose (in accord with an icosahedral packing) the number of tetrahedra per atom equal to five. This is slightly less than the number expected for a space filling distorted tetrahedral packing, but certainly more than the number of pure tetrahedral sites occurring in Bernal's model. Ideally, we should use the decomposition of interstitial sites obtained for a *binary* DRPHS with two size atoms. Unfortunately such data are not available to us. Using five tetrahedra per atom and assuming that there is no chemical short-range order with respect to the distribution of Zr and X atoms, then the average number of *A*₄ tetrahedra per atom is $5x^4$ (*x* is the concentration of *A* in Zr_xX_{1-x}). For a case of tetrahedra built by three *A* plus one *B* atoms the statistical average would be the number of *A*₃ tetrahedra per atom which equals $10x^3(1-x)$. For the matter of chemical short-range order (CSRO) we could introduce a Warren-Cowley-type short-range-order (SRO) parameter α .¹⁵ Then the number of *A*₄ tetrahedra per atom would be given by $5x^4(1+\alpha)^3$. $\alpha < 0$ means preference for unlike neighbors, whereas $\alpha = 0$ describes the random case. For our cases α is unknown. Therefore we start with the random case as a first approximation ($\alpha = 0$). Figure 5 shows the expected number of *A*₄ (Zr_4) tetrahedra per atom as a function of concentration *x* of *A* atoms. Since we observed in the *G*(*r*) functions for Zr_2Pd and Zr_3Rh only changes of the Zr-Zr nearest-neighbor distance with hydriding, we take the *A* atoms to be Zr. The

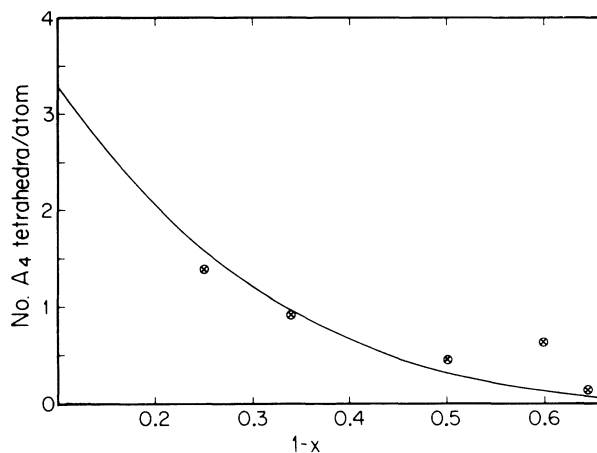


FIG. 5. Solid line shows the predicted number of A_4 (Zr_4) tetrahedral interstitial sites per metal atom as function of concentration *x* in a random amorphous $A_xB_{1-x}(Zr_xX_{1-x})$ alloy containing an average total of five tetrahedral interstitial sites per atom. Experimental data are shown as points and represent the equilibrium hydrogen content obtained for five Zr-based metallic glasses: Zr_3Rh , Zr_2Pd , $Zr_{40}Cu_{60}$ (Ref. 16), $Zr_{36}Ni_{64}$ (Ref. 17), and $ZrNi$ (Ref. 18). All data shown are for 1 atm H_2 and $T = 180-200^\circ C$.

A_4 sites are the tetrahedral sites available for occupancy under normal hydriding conditions. Therefore we plot the experimentally determined concentration of hydrogen-to-metal atoms versus the concentration *x* of Zr atoms in the glassy hydrides on the same graph. Also included are data for $ZrNi$, $Zr_{36}Ni_{64}$, and $Zr_{40}Cu_{60}$ from other groups.¹⁶⁻¹⁸ The agreement between the experimental results and the simple model is excellent with the exception of $Zr_{40}Cu_{60}$. On the other hand, the range of observation is limited to higher Zr concentrations. An extrapolation to a "pure glassy Zr" would lead of course to a H-atom-metal-atom ratio of $c = 5$. However, in order to estimate the maximum H concentration for Zr-rich alloys we must also consider the possibility that H-H interactions may impose severe restrictions on the occupancy of neighboring tetrahedral sites. Our simple model would require modification if such is the case.

From band-structure calculations on crystalline transition-metal hydrides it has been found that, with increasing hydrogen content, a low-lying bonding *s* band occurs.¹⁹ In addition, an antibonding *s* band is observed with energy lying near the Fermi level. The position of the latter band is, for low hydrogen concentrations, nearly independent of the H concentration. For large H concentrations the antibonding *s* band moves upwards in energy. As pointed out first by Switendick, this rise in energy can be viewed in terms of an affective repulsive interaction between closely neighboring hydrogen atoms. A minimum separation between H atoms of 2.1–2.2 Å, is suggested on the basis of the band-structure calculations. Smaller H-H separations lead to a sharp rise in electronic energy and are thus expected to be forbidden. Empirical models of transition-metal hydrides also suggest a minimum allowed hydrogen distance of 2.1–2.2 Å.²⁰ This lower bound for

TABLE II. H-H distances on neighboring sites in a DRPHS model.

| Site No. 1 | Site No. 2 | Configuration | H-H Distance ^a |
|------------|------------|------------------|---------------------------|
| <i>t</i> | <i>t</i> | Common face | 0.408 |
| <i>t</i> | <i>t</i> | Common edge | 0.708 |
| <i>t</i> | <i>t</i> | Common apex | 1.224 |
| <i>t</i> | <i>o</i> | Common face | 0.612 |
| <i>t</i> | <i>o</i> | Common edge | 0.854 |
| <i>t</i> | <i>o</i> | Common apex | 1.319 |
| <i>t</i> | tp | Common top face | 0.704 |
| <i>t</i> | tp | Common side face | ~0.98 |
| <i>t</i> | tp | all other | > 1 |

^aH-H distance measured in units of the nearest-neighbor distance of the atoms defining the polyhedra.

the distance between H neighbors is called the Switendick criterion.

Since the Switendick criterion has been found valid for most hydrided crystalline transition-metal alloys,²¹ we assume its validity also for amorphous transition-metal hydrides. We have therefore calculated the geometrical distances between neighboring tetrahedral sites for a DRPHS model. Table II gives distances for two neighboring polyhedra sites (no. 1 and no. 2), the configuration of the two sites with respect to each other, and the resulting H-H distances obtained if both sites are occupied. For the Zr-based metallic glasses discussed here, the nearest-neighbor distance of the Zr atoms, which are assumed to form the polyhedra, was found experimentally to be $a = 3.35 \text{ \AA}$. In this case, the Switendick criterion excludes simultaneous occupancy of a given site and its neighboring sites if the distance between them is smaller than $0.65a$ from the occupied sites. That means, for example, that a Zr_4 tetrahedron sharing a common face with an occupied tetrahedron, is excluded from being simultaneously occupied. For an exclusively topologically close-packed structure built only from tetrahedra (e.g., Kasper CN12-type structure) the Switendick criterion excludes, for every occupied *t* site, all four neighboring sites. Fortunately each excluded site is itself surrounded by four different additional sites. On the average, each occupied *t* site is accompanied by only one excluded site. Thus we predict that in the hydriding process, only half of the *t* sites in "amorphous Zr" would be available for hydrogen. This suggests that our statistical model, which predicts a maximum of five possible hydrogen sites per metal atom, should be modified to allow a maximum of 2.5 occupied sites per atom in the case of Zr-rich amorphous alloys. For the Zr concentrations we investigated, the repulsive interactions between hydrogen atoms are not as important since we do not reach a large hydrogen concentration. Therefore, it

seems to be worthwhile to investigate the hydrogen absorption capability of glasses with higher Zr concentration. Presumably the model curve in Fig. 5 (given by $5x^4$) should bend over for small x reaching a maximum $[H]/[M]$ value of 2.5 as opposed to 5.

V. CONCLUSION

For Zr-based glassy metal hydrides, the reduced radial distribution functions have been measured and show only a change of the Zr-Zr nearest-neighbor distance with hydriding under normal conditions. With the use of a statistical model based on knowledge of the interstitial sites in glassy metals, the amount of hydrogen absorbed is compared with the number of tetrahedral sites defined by four Zr atoms. Good agreement is found for the known hydrides of ZrX metallic glasses (X is the late transition metal). An upper limit of $[H]/[M] = 2.5$ for the absorption of hydrogen by Zr-rich alloys can then be predicted based on the Switendick criterion for the minimum H-H distance. Neutron-diffraction experiments and further NMR work on metal-glass hydrides of higher Zr content are presently being carried out to test this prediction and to verify the present model for hydrogen site occupancy in the metallic-glass hydrides.

ACKNOWLEDGMENT

The authors would like to thank Dr. Art Williams and Vladimir Matijasevic for their assistance with the x-ray diffraction experiments, and Michael Atzmon, Lowell Hazelton, and Xian Li Yeh for their help with the sample preparation. This work was supported by the U. S. Department of Energy, Project Agreement No. DE-AT03-81ER10870 under Contract No. DE-AM03-76SF00767.

*Permanent address: Universität Göttingen, D-3400 Göttingen, Federal Republic of Germany.

¹X. L. Yeh, K. Samwer, and W. L. Johnson, *Appl. Phys. Lett.* **42**, 242 (1983).

²H. S. Chen and C. E. Miller, *Mater. Res. Bull.* **11**, 49 (1976).

³P. Pietrokowsky, *Rev. Sci. Instrum.* **34**, 445 (1963).

⁴G. S. Cargill III, *Solid State Physics* (Academic, New York, 1975), Vol. 30, p. 227.

⁵R. C. Bowman, M. J. Rosker, and W. L. Johnson, *J. Non-Cryst. Solids* **53**, 105 (1982).

⁶L. Hazelton (unpublished).

⁷K. Kai, T. Fukunaga, T. Nomoto, N. Watanabe, and K. Suzuki, in *Proceedings of the Fourth International Conference on Rapidly Quenched Metals*, edited by K. Suzuki and T. Matsumoto (Japan Institute of Metals, Sendai, 1982), p. 1609.

⁸A. L. Drehman and W. L. Johnson, *Phys. Status Solidi A* **52**,

- 499 (1979).
- ⁹C. D. Gelatt, *Theory of Alloy Phase Formation*, edited by L. D. Bennett (American Institute of Metallurgical Engineers, New York, 1980), p. 456.
- ¹⁰M. Hansen, *Constitution of Binary Alloys (McGraw-Hill, New York, 1958)*, p. 808.
- ¹¹H. Frost, Office of Naval Research Tech. Rep. No. 6, N00014-77-C0002, 1978 (unpublished).
- ¹²R. C. Bowman, Ph.D thesis, California Institute of Technology, Pasadena, 1982 (unpublished).
- ¹³D. G. Westlake, *J. Less-Common Met.* 75, 177 (1980).
- ¹⁴B. Cantor and P. Ramadandrarao, in *Proceedings Fourth International Conference on Rapidly Quenched Metals*, Ref. 7, p. 291.
- ¹⁵B. E. Warren, *X-Ray Diffraction* (Addison-Wesley, Reading, Mass., 1969), p. 229.
- ¹⁶A. M. Maeland, L. Tanner, and G. Libowitz, *J. Less-Common Met.* 74, 1613 (1980).
- ¹⁷S. Hatta, J. Nishioka, and T. Mizoguchi, *Proceedings of the Fourth International Conference on Rapidly Quenched Metals*, Ref. 7, p. 1613.
- ¹⁸K. Aoki, A. Horata, and T. Matsumoto, *Proceedings of the Fourth International Conference on Rapidly Quenched Metals*, Ref. 7, p. 1649.
- ¹⁹A. C. Switendick, Report No. Sand-78-0250, 1978 (unpublished).
- ²⁰P. C. P. Bouten and A. R. Miedema, *J. Less-Common Met.* 71, 147 (1980).
- ²¹K. H. J. Buschow, P. C. Bouten, and A. R. Miedema, *Rep. Prog. Phys.* 45, 937 (1982).